# Enhanced thermoelectric figure of merit in assembled graphene nanoribbons

Liangbo Liang,[1] Eduardo Cruz-Silva,[1,2] Eduardo Costa Girão,[3] and Vincent Meunier[1]
[1]*Department of Physics, Applied Physics, and Astronomy, Rensselaer Polytechnic Institute, Troy, New York 12180, USA*
[2]*Department of Polymer Science and Engineering, University of Massachusetts, Amherst, Massachusetts 01003, USA*
[3]*Departamento de Física, Universidade Federal do Piauí, CEP 64049-550 Teresina, Piauí, Brazil*
(Received 3 July 2012; published 24 September 2012)

Graphene nanowiggles (GNWs) are periodic repetitions of graphene nanoribbon (GNR) junctions resulting in quasi-one-dimensional wiggle-edged structures. They are synthesized using a surface-assisted bottom-up chemical approach and have been predicted to possess unusual electromagnetic properties. Here we show that GNWs also possess superior thermoelectric properties compared to their straight GNR counterparts. We employ a combination of density-functional theory and semiempirical approaches to demonstrate that the presence of wigglelike edges dramatically degrades thermal conductance due to phonons but preserves excellent electronic conduction, resulting in significant enhancement of the thermoelectric figure of merit $ZT$. We show that the resonant tunneling effect between alternate parallel and oblique sectors contributes to maintaining GNR electronic transport properties. We also present a systematic study for a large set of nanowiggle structures to establish how geometry and spin states influence $ZT$ at room temperature, thereby providing a road map for guiding the design and synthesis of specific GNWs for targeted thermoelectric applications.

DOI: 10.1103/PhysRevB.86.115438 PACS number(s): 73.50.Lw, 63.22.Rc, 65.80.Ck, 72.80.Vp

## I. INTRODUCTION

The thermoelectric effect is the direct transformation of temperature gradients into electric voltage and vice versa. This energy conversion mechanism can be used for power generation and refrigeration applications.[1,2] Ideal thermoelectric materials are required to have good electrical conduction to allow facile transport of electrons. At the same time, to avoid the temperature gradient being degraded by heat dissipation, good thermoelectric materials also need to be poor heat conductors. Quantitatively, the thermoelectric conversion efficiency is thus expressed by the dimensionless figure of merit $ZT = S^2 G_e T/k$, where $S$ is the thermal power (or Seebeck coefficient), $T$ is the average temperature, $G_e$ is the electrical conductance, and $k = k_{\mathrm{el}} + k_{\mathrm{ph}}$ is the total thermal conductance, including contributions from electrons $k_{\mathrm{el}}$ and phonons $k_{\mathrm{ph}}$. Much attention has been devoted to finding means to enhance $ZT$. For example, the Seebeck coefficient can be improved by reducing the dimensionality of the system.[3,4] $ZT$ can also be boosted by degrading the thermal conductance due to phonons $k_{\mathrm{ph}}$ and the presence of sharp resonances in the electronic conductance $G_e$.[5,6]

Among new materials under intense scrutiny, graphene has attracted immense interest due to its outstanding thermal properties. For example, a giant Seebeck coefficient (30 mV/K) has been predicted for graphene gated by a sequence of metal electrodes.[7] Further, its superior thermal conductivity has been measured to values as high as 5 kW/mK.[8,9] However, just as pristine graphene is not directly well suited for electronic device applications due to the absence of an electronic band gap, its extremely high thermal conductivity indicates that graphene is not intrinsically a good candidate for thermoelectric devices without tailored modifications. One such modification consists in reducing graphene dimensionality. To that respect, one-dimensional (1D) graphene nanoribbons (GNRs) stand out as better candidates for thermoelectric applications due to their semiconducting behaviors and reduced edge-dependent thermal conductivities.[10] Unfortunately, reported peak $ZT$ values for pristine GNRs at room temperature remain inferior to 0.4,[11] a value shy of what other competing technologies can offer.[2] Clearly, materials science strategies are needed to further degrade thermal conductance while preserving high electronic conductance and thermopower to eventually improve $ZT$. Several approaches have already been examined, such as the use of carbon isotopes,[12] mechanical strain,[13] edge passivation,[14,15] random hydrogen vacancies,[16] atomic vacancies and defects,[4,17,18] molecular junctions,[5] multijunctions GNRs and superlattices,[6,10,11,18] and edge disorder.[19]

Theoretical predictions confirm the great potential of these approaches for enhancing $ZT$. However, most of those modifications also require high experimental control and therefore remain extremely challenging to be realized in the laboratory. In that respect, recent advances in controlled synthesis fuel the hope that some highly tailored modifications of GNR structures can be realized during growth. For example, the synthesis and observation of 1D wigglelike GNRs, called graphene nanowiggles (GNWs), have been achieved with an atomically precise bottom-up approach using surface-assisted coupling of molecular precursors into linear polyphenylenes and their subsequent cyclodehydrogenation.[20] These structures were predicted to possess atypical electronic and magnetic properties, showing a large variation of the band-gap values and the existence of many possible spin distributions, depending on the edge structures.[21,22] Because of the experimental feasibility to synthesize pure GNWs in a controlled way, and thanks to their remarkable electronic properties, it seems now increasingly possible to realize the promises of graphene-based nanostructures for thermoelectric applications.

In this paper, we present a comprehensive study of the thermoelectric properties of a number of GNW structures (Fig. 1). We find that the presence of wiggly edges significantly reduces phonon thermal conductance without appreciably altering electrical transport. The geometrical effects on thermoelectric properties are systematically investigated, offering

 

a guideline for the design of specific GNWs with high $ZT$. The influence of unique magnetic properties of GNWs on $ZT$ is also thoroughly studied.

## II. STRUCTURE AND NOTATION

We adopt the notations introduced in the general framework recently developed to classify nanowiggles according to their geometries, as presented in Ref. 21. Achiral GNWs can be regarded as periodic repetitions of nonaligned armchair- or zigzag-edged GNR sectors seamlessly stitched together without structural defects [Fig. 1(a)]. Parallel and oblique sectors can be either armchair or zigzag edged, leading to four types of GNWs: armchair-armchair (AA), armchair-zigzag (AZ), zigzag-armchair (ZA), and zigzag-zigzag (ZZ). It is convenient to define the width of the parallel ($P_\alpha$) and oblique ($O_\alpha$) sectors by the number of C-C dimer lines ($\alpha = A$) or zigzag strips ($\alpha = Z$) along their width, depending on whether these are armchair or zigzag sectors. Therefore, each structure can be uniquely identified by a ($P_\alpha$,$O_\beta$)$\equiv \alpha\beta$-PO notation. For instance, the nanowiggles reported experimentally[20] are made of armchair parallel and armchair oblique sectors (type AA) with widths corresponding to ($9_A$,$6_A$), hence denoted as AA-96 [Fig. 1(b)]. Examples of AZ-74, ZA-49, and ZZ-64 are also presented in Fig. 1.

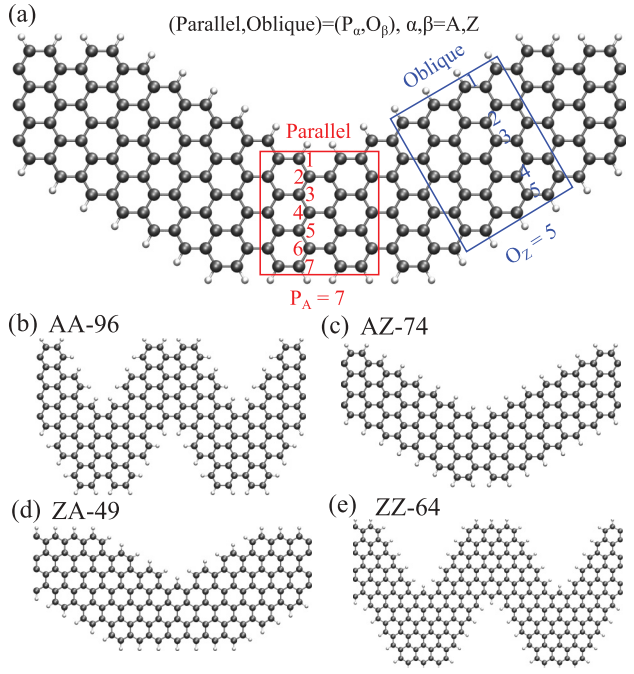


FIG. 1. (Color online) (a) Geometry and identifying notation of a hydrogen-passivated GNW made up of successive parallel and oblique sectors of armchair (A) or zigzag (Z) edge geometries. Here, a specific GNW made up of armchair-edged parallel sectors and zigzag-edged oblique sectors is shown. Using the conventional notation for straight nanoribbons,[21] the width of the armchair-edged parallel sector is identified as $P_A = 7$ and the width of the zigzag-edged oblique sector is $O_Z = 5$, resulting in a AZ-75 notation. (b)–(e) Examples of AA-96, AZ-74, ZA-49, and ZZ-64 GNWs, respectively. All the GNWs are periodic in the horizontal direction.

## III. METHODOLOGY

Thermoelectric properties are obtained after the computation of the ballistic transport properties of electrons and phonons.[5,23] The ballistic phonon thermal conductance $k_{ph}$ is evaluated using the following Landauer-type formula:[23,24]

$$k_{ph} = \frac{\hbar^2}{2\pi k_B T^2}\int_0^\infty d\omega\omega^2 T_{ph}(\omega)\frac{e^{\hbar\omega/k_BT}}{(e^{\hbar\omega/k_BT}-1)^2}, \quad (1)$$

where the phonon transmission function $T_{ph}(\omega)$ is obtained using density-functional theory (DFT) combined with the nonequilibrium Green's function (NEGF) formalism.[5] In the specific case of 1D systems, $T_{ph}(\omega)$ is simply given by the number of phonon modes at frequency $\omega$. It can be seen from Eq. (1) that, at low temperatures, low-frequency modes have dominating contributions to the thermal conductance.

Similarly, the electron transmission function $T_{el}(E)$ leads to the computation of the following integral:[25]

$$K_n(\mu) = \frac{2}{h}\int_{-\infty}^{\infty} dE T_{el}(E)(E-\mu)^n\left(-\frac{\partial f(E,\mu)}{\partial E}\right), \quad (2)$$

where $f(E,\mu) = 1/(1+e^{(E-\mu)/k_BT})$ is the Fermi-Dirac distribution function evaluated at chemical potential $\mu$. Similar to the phonon transmission, $T_{el}(E)$ is defined as the number of electronic bands crossing energy $E$ for 1D systems. The integrals in the above equations are very sensitive to the electronic bands around the Fermi energy and provide all the quantities needed to evaluate $ZT$: $G_e = e^2K_0(\mu)$, $S = K_1(\mu)/[eTK_0(\mu)]$, and $k_{el} = \{K_2(\mu) - [K_1(\mu)]^2/K_0(\mu)\}/T$. Finally, the thermoelectric figure of merit $ZT$ can be obtained by

$$ZT = \frac{S^2G_eT}{k_{el}+k_{ph}}. \quad (3)$$

The formalism to compute $ZT$ has been implemented using the electron and phonon transmission functions $T_{el}(E)$ and $T_{ph}(\omega)$, which are obtained by counting the number of bands at a given electronic energy or phonon frequency from the full electron and phonon band structures of the system, respectively. For example, to obtain accurate full electron and phonon band structures for the systems depicted in Fig. 1, plane-wave DFT calculations were performed using the VASP package[26,27] within the generalized gradient approximation (GGA) using the Perdew-Burke-Enzerhof (PBE) exchange-correlation functional.[28] The electronic band structures are computed after full atomic relaxation until the residual forces are below 0.01 eV/Å, using a fine $k$-point Brillouin-zone sampling and projector augmented wave (PAW) pseudopotentials, with a cutoff energy of 400 eV for the plane-wave basis set. For phonon calculations, a supercell constructed from the optimized unit cell is used by VASP to generate the force constant matrix in the finite displacement scheme. Then the PHONOPY code was utilized to obtain the phonon dispersion over the whole Brillouin zone.[29]

We have used this DFT-based approach to evaluate the thermoelectric properties of a number of GNW systems (Figs. 2 and 3). However, DFT is too computationally demanding to perform a systematic study of the relationship between the details of the geometry and the thermoelectric properties of GNWs of any size. Therefore a less expensive self-consistent $\pi$

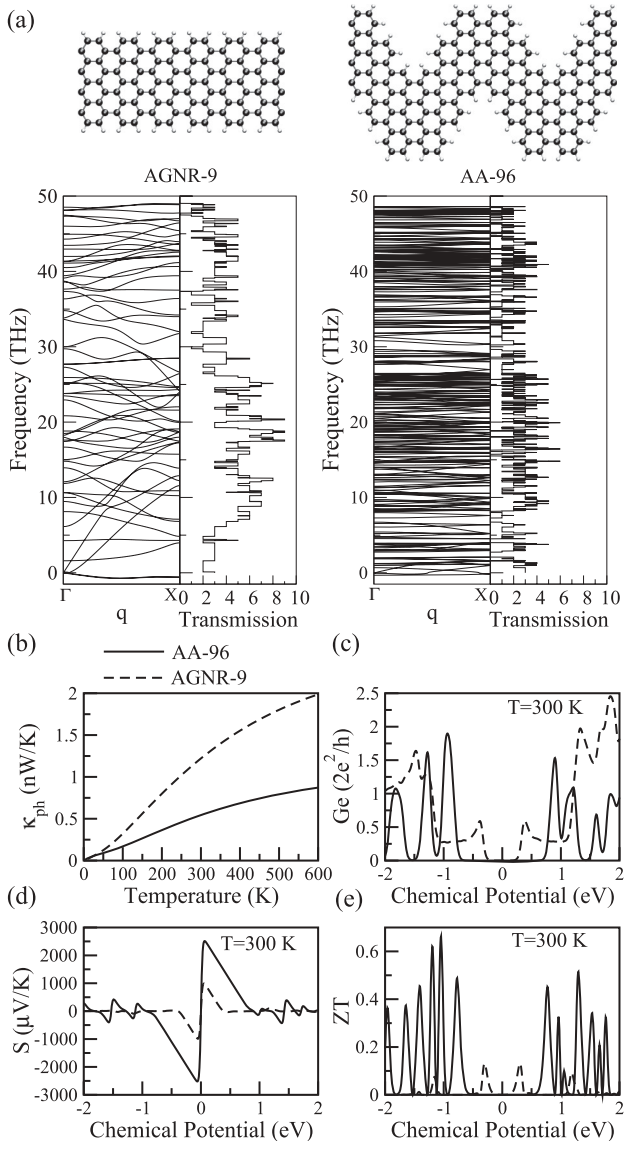


FIG. 2. (a) Phonon dispersions and transmission functions of AGNR-9 (left) and AA-96 (right) with their structures schematically provided on the top. AGNR-9 is the straight counterpart to AA-96 sharing the same width. (b) Thermal conductance $k_{ph}$ vs temperature of AA-96 (solid line) and AGNR-9 (dashed line). (c) Electrical conductance $G_e$. (d) Thermal power $S$. (e) Thermoelectric figure of merit $ZT$ vs chemical potential $\mu$ at room temperature ($T = 300$ K) of AA-96 (solid line) and AGNR-9 (dashed line). The zero in the chemical potential is chosen at the Fermi level. All calculations here are done within DFT and both structures are in their paramagnetic (PM) state.

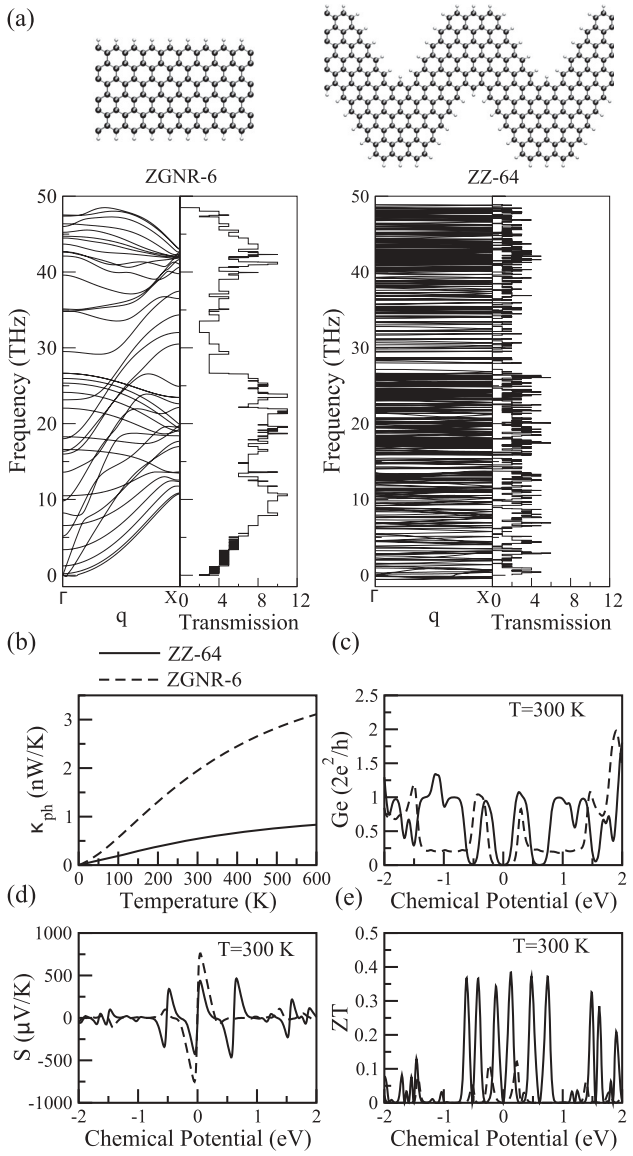


FIG. 3. (a) Phonon dispersions and transmissions functions of ZGNR-6 (left) and ZZ-64 (right) with their structures schematically shown on the top. ZGNR-6 is the straight counterpart to ZZ-64. (b) Thermal conductance $k_{ph}$ vs temperature of ZZ-64 (solid line) and ZGNR-6 (dashed line). (c) Electrical conductance $G_e$. (d) Thermopower $S$. (e) Thermoelectric figure of merit $ZT$ vs chemical potential $\mu$ at room temperature ($T = 300$ K) of ZZ-64 (solid line) and ZGNR-6 (dashed line). The zero in the chemical potential is chosen at the Fermi level. All calculations here are done by DFT and both structures are in an antiferromagnetic (AFM) state.

band tight-binding $+U$ (TBU) model has been used to perform a systematic description of electronic and magnetic properties of GNWs and GNRs systems.[21] First-, second-, and third-nearest-neighbor hopping integrals are given by $t_1 = 3.2$ eV, $t_2 = 0.0$ eV, and $t_3 = 0.3$ eV, respectively. The different coordination number at the edges is accounted for by including a $\Delta t_1 = 0.2$ eV correction to the $t_1$ parameter for the frontier atoms.[30] The $U$ parameter is parameterized on DFT-PBE calculations as $0.92t_1$ to describe the magnetic interaction.[21] Furthermore, compared to DFT, a less expensive density-functional based tight-binding method (DFTB+)[31] is used to build force constant matrices and compute phonon transmission functions. This combination of TBU and DFTB+ (referred to TB below) yields $ZT$ values in excellent agreement with DFT calculations, as exemplified by the case study shown in Fig. 4.

## IV. RESULTS AND DISCUSSION

### A. AA GNWs

Figure 2(a) shows DFT-calculated phonon dispersions and corresponding transmission functions of AA-96 and its straight

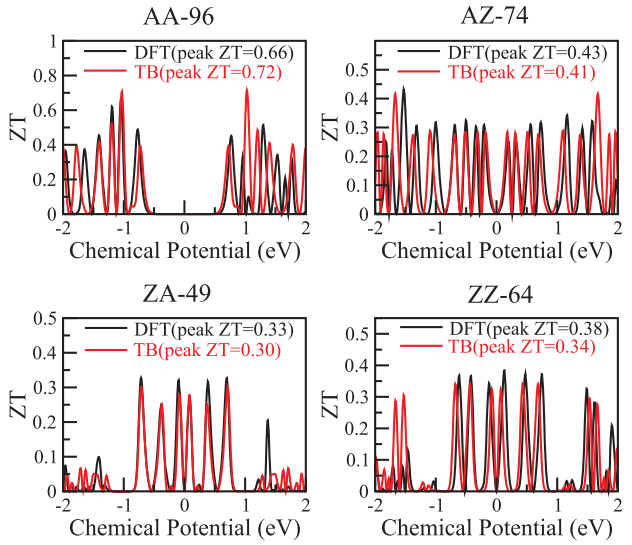


FIG. 4. (Color online) $ZT$ vs $\mu$ at $T = 300$ K obtained both by DFT (black) and TB (red) for AA-96, AZ-74, ZA-49, and ZZ-64 GNWs depicted in Fig. 1. Except AA-96 in the PM state, others are all in the AFM state.

counterpart AGNR-9 in their paramagnetic (PM) state. We do not have to worry about other possible magnetic states since, like armchair GNRs (AGNRs), AA GNWs only exist in a PM configuration.[21] Note that phonon modes at ∼94 THz (∼3140 $cm^{-1}$) corresponding to C-H modes[32] are not shown and they make little contribution to thermal conductance. Note also that the lowest phonon modes in both nanoribbon and nanowiggle are found to show slightly negative (imaginary) frequencies, indicating instability from inherent edge stresses.[15] These small numerical issues at extremely low-frequency modes can be eliminated for the most part by using a larger supercell with extremely high precision (but at tremendous computational costs). They are found not to be detrimental to the accuracy of thermal conductance calculations. It can be readily seen that the nanoribbon exhibits more dispersive phonon branches than the nanowiggle, generally resulting in larger values of $T_{ph}(\omega)$. The existence of a large number of flat phonon bands in AA-96 gives its $T_{ph}(\omega)$ more frequencies that do not contribute to thermal transport compared to AGNR-9. Therefore, the thermal conductance of the nanowiggle is substantially lower than that of the nanoribbon as clearly seen in Fig. 2(b). As a result, at room temperature, the straight AGNR-9 has a thermal conductance of 1.22 nW/K while the nanowiggle's thermal conductance is decreased to 0.54 nW/K. Such spectacular suppression of phonon transmission and corresponding reduction of thermal conductance arise from the wigglelike edges acting as scattering centers and the mismatch of phonon modes in the parallel and oblique sectors.[6] Conversely, the wigglelike edges do not significantly disrupt electrical conduction [Figs. 2(c) and 2(d)]. Consequently, in the chemical potential region (−1.20 eV, 1.20 eV) where peak $ZT$ values are produced, peak $G_e$ values of AA-96 are larger than those of AGNR-9. Figure 2(c) also shows that a larger electronic band gap (1.48 eV) develops in the electrical conductance of AA-96, compared to the band gap (0.58 eV) of AGNR-9. Since a large electronic band gap can yield high thermopower values,[6] AA-96 exhibits higher $S$ than AGNR-9 [Fig. 2(d)]. This, combined with the preserved electrical conductance $G_e$ and degraded phonon thermal conductance, leads to a high peak with $ZT$ value 0.66 at $\mu = -1.08$ eV [to be compared to 0.13 in Fig. 2(e) for corresponding AGNR-9], in excellent agreement with the study of Chen *et al.*[11]

### B. ZZ GNWs

In contrast to AGNRs, it is established that straight zigzag GNRs (ZGNRs) in the PM configuration have a zero electronic band gap. The metallic behavior results in the mutual cancellation of electron and hole contributions to $S$, leading to very small values of $S$ and subsequently almost zero $ZT$ values for all widths.[10,19] Our calculations show that ZGNR-6 [Fig. 3(a)] in the PM state has a peak $ZT$ value of only 0.08 at room temperature (not shown). Clearly, opening a band gap is necessary to enhance $ZT$ in ZGNRs. ZGNRs' electronic ground state is antiferromagnetic (AFM). The presence of an AFM spin ordering breaks the symmetry of the spin distribution and opens a band gap of 0.40 eV for ZGNR-6 [Fig. 3(c)] and gives a corresponding $ZT$ peak of 0.12 [shown as a dashed line in Fig. 3(e)]. To further increase $ZT$, thermal conductance needs to be reduced. Similar to AA nanowiggles, the wigglelike edges in ZZ systems also cause much less dispersive phonon branches compared to their straight GNR counterparts and thus generally smaller values of transmission functions [Fig. 3(a)]. As a result, $k_{ph}$ of ZZ-64 is dramatically reduced, as shown in Fig. 3(b). At room temperature, ZZ-64 in the AFM spin ordering has a thermal conductance of 0.54 nW/K while ZGNR-6 shows $k_{ph}$ as high as 1.95 nW/K. Similar reduction of $k_{ph}$ is observed for ZZ-64 in the PM state as well (not shown). In addition, the particular edge structure opens up a band gap of 0.12 eV for the nanowiggle even in the PM state, indicative to a larger thermopower $S$. Indeed, at room temperature, the peak $S$ of PM ZGNR-6 is only 97.06 $\mu$V/K but PM ZZ-64 has a $S$ peak of 477.94 $\mu$V/K. The substantial reduction of $k_{ph}$ with enhanced power factor $S^2G_e$ enables the peak $ZT$ of ZZ-64 in the PM configuration reaching 0.36 (not shown), more than four times that (0.08) of PM ZGNR-6. AFM spin ordering, the most stable magnetic state according to our previous calculations,[21] opens the band gap to 0.26 eV for ZZ-64 [Fig. 3(c)], resulting in the peak $ZT$ of 0.38 at room temperature [solid line in Fig. 3(e)].

### C. Electronic resonant tunneling

Turning to the two other types of nanowiggles AZ and ZA, DFT calculations also show flat phonon branches and reduced thermal conductance. For example, at room temperature, AZ-74 and ZA-49 have $k_{ph}$ as 0.66 and 0.62 nW/K, respectively. It is important to note that many strategies, such as the introduction of atomic vacancies and Stone-Wales defects, have been proposed to degrade phonon thermal conductance but failed to enhance $ZT$ significantly because electrical conductance and thermopower are suppressed as well, as reported by Mazzamuto *et al.*[18] Here, nanowiggles are able to have phonon thermal conductance suppressed while essentially preserving electronic conduction [Figs. 2(c),

2(d), 3(c), and 3(d)], due to electronic resonant tunneling. In a nanowiggle composed of alternate parallel and oblique sectors, the parallel sectors act as barriers between oblique sectors, and vice versa. In other words, a GNW can be seen as a multibarrier system, where a resonant tunneling transport may occur and induce strong oscillations of the electrical conductance and thermopower.[6,33] From Figs. 2(c) and 2(d), in comparison to AGNR-9, oscillations (multiple peaks) of the electrical conductance and thermopower of AA-96 (solid line) are clearly present, indicating the existence of resonant tunneling. Those peaks are directly responsible for multiple $ZT$ peaks in Fig. 2(e). Similar oscillations of the electrical conductance and thermopower can be seen in Figs. 3(c) and 3(d) as well for ZZ-64, resulting in multiple peaks of $ZT$ close to the Fermi level in Fig. 3(e). Such resonant tunneling effect not only preserves electrical conduction, but also leads to multiple $ZT$ peaks so that good thermoelectric performance can occur at many chemical potential values. In contrast, straight GNRs show few significant $ZT$ peaks close to Fermi level [see dashed line plots in Figs. 2(e) and 3(e)].

### D. Systematic study: establishing a road map to optimal $ZT$ in GNWs

The DFT calculations above clearly demonstrate that nanowiggles have superior thermoelectric performance compared to conventional nanoribbons. It is known that geometry has a great influence on electronic properties of nanowiggles[21] and the results shown above indicate that thermal conductance is sensitive to geometry as well. It is therefore of great importance to systematically study geometry effects on thermoelectric properties of nanowiggles. However, as pointed out earlier, DFT is too computationally expensive for a comprehensive study and a less expensive TB approximation has been adopted to provide a systematic way to compute $ZT$ for a large range of structures. Four particular nanowiggle structures [see Figs. 1(b)–1(e)] have been chosen for both DFT and TB calculations for benchmarking purposes and a remarkable agreement between their results is found (Fig. 4), indicating that TB can be used for the systematic study we will present now.

The charts shown in Fig. 5 describe how peak $ZT$ values vary with respect to the widths of parallel ($P$) and oblique ($O$) sectors for AA nanowiggles in the PM state, and for AZ, ZA, and ZZ nanowiggles in the AFM state. We chose those spin configurations since only the PM spin ordering exists for AA GNWs and the AFM state is the most stable spin configuration for nanowiggles containing zigzag edges.[21,22] Each square represents the highest $ZT$ peak value for a specific GNW structure, with the chemical potential ranging from $-2$ to 2 eV at room temperature. Due to the dependence of $ZT$ on both electric and thermal conduction, it exhibits complex relations to geometrical parameters $P$ and $O$. In general, our calculations predict that $k_{\mathrm{ph}}$ gradually increases with the increase of $P$ and $O$ while electronic band gap decreases when the size of a structure gets larger. Therefore, small $ZT$ values are usually found in the upper-right portion of each graph where $P$ and $O$ are the largest, while $ZT$ values exceeding a half of unity appear mainly in the lower-left area of each graph. In addition to this general rule, for AA GNWs in Fig. 5(a), our recent work

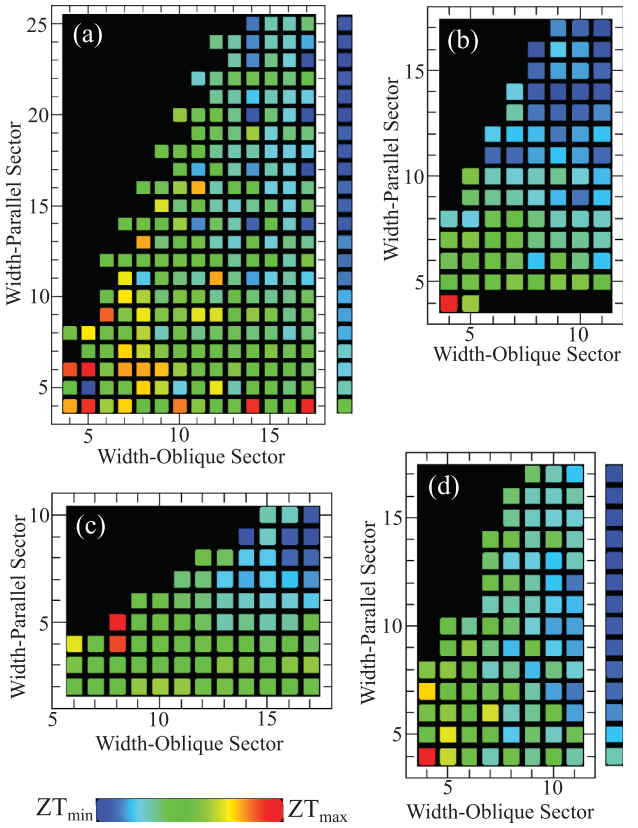


FIG. 5. (Color online) Peak $ZT$ (room temperature) as a function of the widths of parallel (P) and oblique sectors (O) for (a) AA GNWs in the PM state and for (b) AZ, (c) ZA, and (d) ZZ GNWs in the AFM state. The points absent mainly on the upper-left corner of each graph correspond to geometries not allowed by the particular choice for P and O. In (a), the column on the right side of the frame represents peak $ZT$ values of AA GNWs' straight counterparts in the PM state. Similarly in (d), the column next to the frame shows peak $ZT$ of ZZ GNWs' straight counterparts in the AFM state. In these charts, minima and maxima of peak $ZT$ values are (a) $ZT_{\mathrm{min}} = 0.04$, $ZT_{\mathrm{max}} = 0.79$; (b) $ZT_{\mathrm{min}} = 0.12$, $ZT_{\mathrm{max}} = 0.65$; (c) $ZT_{\mathrm{min}} = 0.07$, $ZT_{\mathrm{max}} = 0.56$; and (d) $ZT_{\mathrm{min}} = 0.04$, $ZT_{\mathrm{max}} = 0.57$.

shows[21] that electronic band gaps can be classified according multiple-of-three rules like straight AGNRs. The band gap $\Delta_N$ for AGNRs with $N = (3i + j)$ C-C lines follows the relation $\Delta_{3i+1} > \Delta_{3i} > \Delta_{3i+2}$, indicating that structures with $\mathrm{mod}(\mathrm{P_A},3) = \mathrm{mod}(\mathrm{O_A},3) = 2$ possess the smallest band gaps. Generally, in these structures, small band gaps lead to small values of thermopower and therefore small $ZT$ values [shown in Fig. 5(a) evenly spaced in units of 3]. For many other systems, the existence of large band gaps (up to 1.7 eV) results in large thermopower values and $ZT$ values usually higher than 0.5, indicating that AA GNWs are the best candidates as thermoelectrics among all four types of nanowiggle systems. Although straight AGNRs possess similarly large band gaps, the considerably higher thermal conductance renders their peak $ZT$ values significantly smaller, as demonstrated in the column of data shown on the right side of the frame in Fig. 5(a). With the notable exception of very narrow AGNRs ($P < 8$), the peak $ZT$ value quickly decreases as $P$ increases. Similar results can be observed in Fig. 5(d) where peak $ZT$

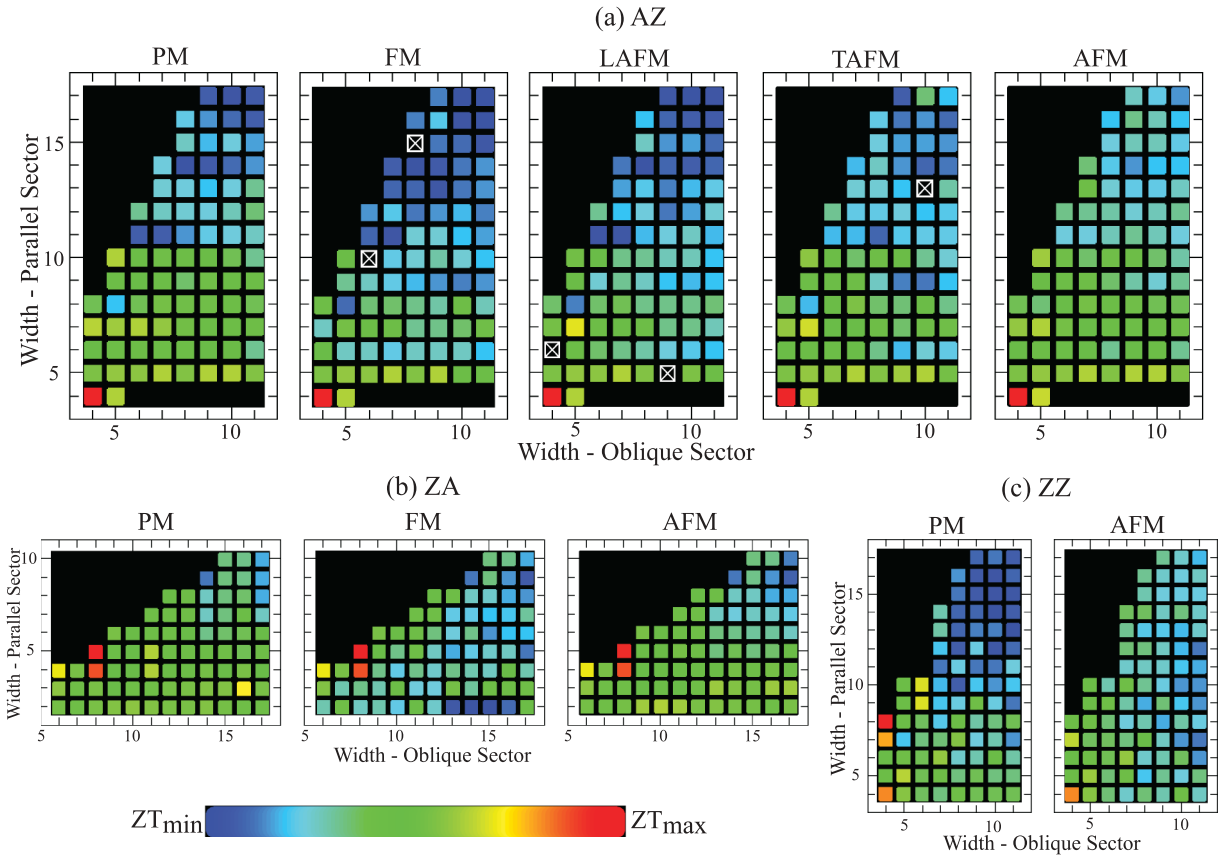


FIG. 6. (Color online) Peak $ZT$ (room temperature) as a function of P and O for (a) AZ GNWs in the PM, FM, LAFM, TAFM, and AFM state, respectively, for (b) ZA GNWs in the PM, FM, and AFM state, respectively, and for (c) ZZ GNWs in the PM and AFM state, respectively. Conventional FM spin ordering cannot be found for most ZZ GNWs[21] and hence $ZT$ corresponding to the FM state is not shown here. A system that does not possess a particular magnetic state is marked by a cross. In these charts, minima and maxima of peak $ZT$ values are (a) $ZT_{\min} = 0.02$, $ZT_{\max} = 0.65$; (b) $ZT_{\min} = 0.02$, $ZT_{\max} = 0.57$; and (c) $ZT_{\min} = 0.03$, $ZT_{\max} = 0.65$.

values of straight ZGNRs (shown as a column of data next to the frame) are much smaller than those of their nanowiggle counterparts.

The presence of domains with varying chirality leads to the emergence of a rich variety of spin-dependent properties in GNWs with at least one zigzag type of edge. For instance, in addition to conventional paramagnetic (PM), ferromagnetic (FM), and antiferromagnetic (AFM) spin configurations, AZ systems exhibit two more metastable states: longitudinal antiferromagnetic (LAFM) and transantiferromagnetic (TAFM).[21,22] We examine the influence of the magnetic states on $ZT$ in Fig. 6. Unlike straight ZGNRs for which peak $ZT$ values in the PM state are nearly zero for all widths due to the absence of band gap, unique wigglelike edges help to open a band gap (up to 1.5 eV) for many nanowiggle structures in the PM state, especially for those with small $P$ and $O$. Combined with reduced $k_{\text{ph}}$, they usually possess peak $ZT$ values exceeding 0.5 in the PM state at room temperature, as shown in the lower-left corners of the charts corresponding to the PM state in Fig. 6. However, when $P$ and $O$ are large enough, the band gap progressively vanishes, leading to small $ZT$ values. Conversely, the introduction of spin ordering, particularly AFM, opens a band gap around 0.3 eV and generally increases $ZT$ again, as presented in the upper-right areas of the charts shown in Fig. 6. On the other hand, the FM magnetic configuration usually leads to symmetric electronic transmission around the Fermi level and the mutual cancellation of electron and hole contributions to $S$, subsequently decreasing peak $ZT$ values, as shown in the upper-right areas of FM charts in Figs. 6(a) and 6(b).

Because thermoelectric devices usually operate at room or higher temperature, it is important to note that the AFM spin ordering, where the highest $ZT$ usually occurs among all magnetic states, remains intact at room temperature for most nanowiggle systems, since DFT calculations reveal that the AFM state is generally more stable than the PM state by more than 50 meV,[21] indicating the barrier energy for the transition from AFM to PM is higher than the room-temperature thermal energy. Conversely, other spin states, especially FM, are likely to be destroyed at room temperature.

## V. CONCLUSION

In summary, because of the particular periodic arrangement of oblique and parallel graphene patches, GNWs are found to possess significantly enhanced thermoelectric performance

compared to their straight GNRs counterparts. Such improvement originates from the combination of (i) reduced phonon thermal conductance due to phonon scattering by wigglelike edges and the mismatch of phonon modes in the parallel and oblique sectors and (ii) the electron resonant tunneling effect between these sectors which guarantee good electronic conduction. In general, the peak $ZT$ value of AA GNWs is more than triple that of straight AGNRs of the same width. For many GNWs with at least one zigzag sector, the interplay between the effects of parallel and oblique sectors opens a band gap, leading to larger thermopower and consequently to higher $ZT$ while peak $ZT$ values of straight ZGNRs are almost zero due to their metallicity. Among all nanowiggle structures studied here, AA-65 has the maximum $ZT = 0.79$ at room temperature. A large proportion of AA systems possess $ZT$ higher than 0.5 in comparison to the other three types of achiral GNWs, leading to the conclusion that the experimentally available AA GNWs are the most promising candidates for thermoelectric applications. Finally, our systematic study of the effects of geometry and spin distribution on $ZT$ provides a guideline for the experimental design and synthesis of specific GNWs for thermoelectric applications.

We note that nonlocal hybrid and screened hybrid exchange-correlation functionals are expected to provide a better description of the electronic properties of graphene-based materials compared to the semilocal PBE functional used here.[34] However, our findings based on the PBE about superior $ZT$ values of wigglelike GNWs compared to straight GNRs should remain qualitatively or even semiquantitatively correct. The conclusions about the geometrical influence and magnetic effects on $ZT$ are not expected to be altered either.

Note also that all the systems investigated here were considered as free-standing, and no substrate effects were included. To make a practical thermoelectric device, a GNW would need to be deposited on a substrate and coupled with heat and electron reservoirs, which may influence significantly the electronic and phonon behaviors. In that respect, our recent calculations show that the gold substrate on which GNWs are assembled does have a considerable effect on their electronic properties. In addition, it is known that a substrate may act as a phonon-scattering center that can further reduce the phonon thermal conductance of the adsorbate.[4] It will be a valuable objective of future works to study how the environment affects the thermoelectric performance of a GNW, especially with ever increasing computational resources available in the future.

## ACKNOWLEDGMENTS

We acknowledge illuminating discussions with Prof. Mildred Dresselhaus and Prof. Roman Fasel. LL and VM are supported by New York State under NYSTAR Contract No. C080117. E.C.S. was supported in part by Polymer based materials for Harvesting Solar Energy (PHASE), an Energy Frontier Research Center (EFRC) funded by the U.S. Department of Energy (DOE) under Award No. DE-SC0001087. ECG acknowledges the Brazilian agencies CAPES (Coordenação de Aperfeiçoamento de Pessoal de Nível Superior) for the sandwich program fellowship (Process No. 0327-10-7), CNPq (Conselho Nacional de Desenvolvimento Científico e Tecnológico) (Process No. 140887/2008-3) and FUNCAP (Fundação Cearense de Apoio ao Desenvolvimento Científico e Tecnológico) (PRONEX PR2-0054-00022.01.00/11). VM is also grateful for the support from the Center for Nanophase Materials Sciences (CNMS), sponsored at Oak Ridge National Laboratory by the Division of Scientific User Facilities, U.S. DOE. All the calculations were performed on resources from the Computational Center for Nanotechnology Innovation at Rensselaer Polytechnic Institute (RPI).

[1] L. Bell, Science **321**, 1457 (2008).
[2] C. Vining, Nat. Mater. **8**, 83 (2009).
[3] M. Dresselhaus, G. Chen, M. Tang, R. Yang, H. Lee, D. Wang, Z. Ren, J. Fleurial, and P. Gogna, Adv. Mater. **19**, 1043 (2007).
[4] T. Gunst, T. Markussen, A. P. Jauho, and M. Brandbyge, Phys. Rev. B **84**, 155449 (2011).
[5] K. K. Saha, T. Markussen, K. S. Thygesen, and B. K. Nikolić, Phys. Rev. B **84**, 041412 (2011).
[6] F. Mazzamuto, V. HungNguyen, Y. Apertet, C. Caër, C. Chassat, J. Saint-Martin, and P. Dollfus, Phys. Rev. B **83**, 235426 (2011).
[7] D. Dragoman and M. Dragoman, Appl. Phys. Lett. **91**, 203116 (2007).
[8] A. Balandin, S. Ghosh, W. Bao, I. Calizo, D. Teweldebrhan, F. Miao, and C. Lau, Nano Lett. **8**, 902 (2008).
[9] J. Seol, I. Jo, A. Moore, L. Lindsay, Z. Aitken, M. Pettes, X. Li, Z. Yao, R. Huang, D. Broido, N. Mingo, R. Ruoff, and L. Shi, Science **328**, 213 (2010).
[10] W. Huang, J. S. Wang, and G. Liang, Phys. Rev. B **84**, 045410 (2011).
[11] Y. Chen, T. Jayasekera, A. Calzolari, K. Kim, and M. Buongiorno Nardelli, J. Phys.: Condens. Matter **22**, 372202 (2010).
[12] N. Mingo, K. Esfarjani, D. A. Broido, and D. A. Stewart, Phys. Rev. B **81**, 045408 (2010).
[13] N. Wei, L. Xu, H. Wang, and J. Zheng, Nanotechnology **22**, 105705 (2011).
[14] J. Hu, S. Schiffli, A. Vallabhaneni, X. Ruan, and Y. Chen, Appl. Phys. Lett. **97**, 133107 (2010).
[15] Z. Tan, J. Wang, and C. Gan, Nano Lett. **11**, 214 (2011).
[16] X. Ni, G. Liang, J. Wang, and B. Li, Appl. Phys. Lett. **95**, 192114 (2009).
[17] J. Haskins, A. Kinaci, C. Sevik, H. Sevincli, G. Cuniberti, and T. Cagin, ACS Nano **5**, 3779 (2011).
[18] F. Mazzamuto, J. Saint-Martin, V. Nguyen, C. Chassat, and P. Dollfus, J. Comput. Electron. **11**, 67 (2012).
[19] H. Sevinçli and G. Cuniberti, Phys. Rev. B **81**, 113401 (2010).
[20] J. Cai, P. Ruffieux, R. Jaafar, M. Bieri, T. Braun, S. Blankenburg, M. Muoth, A. Seitsonen, M. Saleh, X. Feng, K. Mullen, and R. Fasel, Nature (London) **466**, 470 (2010).
[21] E. C. Girão, L. Liang, E. Cruz-Silva, A. Filho, and V. Meunier, Phys. Rev. Lett. **107**, 135501 (2011).
[22] E. C. Girão, E. Cruz-Silva, L. Liang, A. G. Souza Filho, and V. Meunier, Phys. Rev. B **85**, 235431 (2012).

[23]N. Mingo and D. A. Broido, Phys. Rev. Lett. **95**, 096105 (2005).
[24]L. G. C. Rego and G. Kirczenow, Phys. Rev. Lett. **81**, 232 (1998).
[25]K. Esfarjani, M. Zebarjadi, and Y. Kawazoe, Phys. Rev. B **73**, 085406 (2006).
[26]G. Kresse and J. Furthmüller, Comput. Mater. Sci. **6**, 15 (1996).
[27]G. Kresse and J. Furthmüller, Phys. Rev. B **54**, 11169 (1996).
[28]J. P. Perdew, K. Burke, and M. Ernzerhof, Phys. Rev. Lett. **77**, 3865 (1996).
[29]A. Togo, F. Oba, and I. Tanaka, Phys. Rev. B **78**, 134106 (2008).
[30]D. Gunlycke and C. T. White, Phys. Rev. B **77**, 115116 (2008).
[31]D. Porezag, T. Frauenheim, T. Köhler, G. Seifert, and R. Kaschner, Phys. Rev. B **51**, 12947 (1995).
[32]R. Gillen, M. Mohr, J. Maultzsch, and C. Thomsen, Phys. Rev. B **80**, 155418 (2009).
[33]G. D. Guttman, E. Ben-Jacob, and D. J. Bergman, Phys. Rev. B **51**, 17758 (1995).
[34]V. Barone, O. Hod, J. Peralta, and G. Scuseria, Acc. Chem. Res. **44**, 269 (2011).